

Solution Synthesis and Characterization of Size-Controlled $\text{Fe}_3\text{O}_4@ \text{SiO}_2$ Magnetic Nanoparticles for Nucleic Acid Analysis

Rakesh Kumar Gupta¹, Shikha Vishwakarma¹, Prachi Tadge^{1*} and Sudeshna Ray^{1*}

¹Advanced Materials Research Centre, Faculty of Science, Rabindranath Tagore University, Bhopal, India

Abstract - Due to the presence of distinctive magnetic response, a chemically changeable surface, and minimal cytotoxicity, $\text{Fe}_3\text{O}_4@ \text{SiO}_2$ magnetic nanoparticles have attracted significant attention in the biomedical field. In this work, we report the synthesis of Fe_3O_4 nanoparticles using a solvothermal mediated method using $\text{FeCl}_3 \cdot 6\text{H}_2\text{O}$, sodium acetate and poly ethylene glycol (PEG-6000). The pH of the suspension found to have a pronounced impact on the size and the shape of the synthesized Fe_3O_4 NPs. Using a modified Stöber technique, $\text{Fe}_3\text{O}_4@ \text{SiO}_2$ magnetic nanoparticles have been prepared, followed by the synthesis of streptavidin (SA) Immobilized Onto SA- $\text{Fe}_3\text{O}_4@ \text{SiO}_2$ NPs. Due to the effective SA immobilization, the synthesized nanoparticles exhibit a great attractive transporters for nucleic corrosive discovery.

1. Introduction

Due to their distinctive physical and chemical characteristics and the numerous potential applications in the bio and environmental domains, magnetic nanoparticles have gained more interest in research over the past ten years [1, 2]. One of the most significant magnetic nanomaterials is the magnetic nanoparticle (NP) [3, 4]. Numerous articles have described the synthesis of various functional magnetic NPs up to this point. $\text{Fe}_3\text{O}_4@ \text{SiO}_2$ magnetic NPs have good bio-separation, enzyme immobilization, diagnostic, and therapeutic properties. They also have a distinctive magnetic response, a chemically changeable surface, and minimal cytotoxicity [7–9]. Magnetic NPs made of Fe_3O_4 and $\text{Fe}_3\text{O}_4@ \text{SiO}_2$ has a lengthy history of preparation. Their synthesis can be done in a number of ways, including physical mechano-grinding, gas phase vapour deposition, and aqueous solution-based methods such as micro-emulsion, the sol-gel

technique, and co-precipitation of ferrous and ferric salts [10–12]. As far as we are aware, the solvothermal technique is a common method for creating nanoscale materials with precise control their size, shape, crystal plane, and electrochemical properties [13].

The solvothermal technique has been used to successfully produce a variety of Fe_3O_4 morphologies during the past few decades, including nanospheres [14–16] nanocubes [17–18] nanowires [19–20] nanooctahedral [23–24] nanotubes [25–26] nanoplates [27–28] and nanoprisms [29–30]. Restrictive solvothermal synthesis of Fe_3O_4 NPs with adjustable size and magnetic saturation value was also accomplished. By combining $\text{FeCl}_3 \cdot 6\text{H}_2\text{O}$, ethylene glycol (EG), sodium acetate (NaAc), and polyethylene glycol (PEG) at 453 K or higher temperature, Cheng and colleagues have reported a simple solvothermal system to sustain Fe_3O_4 NPs. In such a system, the molecular weight or dosage of PEG could be used to adjust the average grain size of the Fe_3O_4 NPs while the Fe^{3+} concentration could be used to adjust the diameter of the particles [31]. Moreover, the $\text{Fe}_3\text{O}_4 @ \text{SiO}_2$ NPs demonstrated great biocompatibility and extensive use when the Fe_3O_4 NPs were enclosed in a silica shell while still maintaining a high magnetic saturation value [32]. The Stöber procedure is one of the well-known methods for coating a silica layer on Fe_3O_4 NPs.

According to the solvothermal system described above with a sequential (pH) value, Fe_3O_4 NPs with adjustable diameters were successfully synthesized in this study, and the mechanism of the particle formation was explained. Adapting modified Stöber procedure, $\text{Fe}_3\text{O}_4 @ \text{SiO}_2$ NPs were effectively produced. Investigation of the magnetic characteristics of Fe_3O_4 NPs was carried out and the use of $\text{Fe}_3\text{O}_4 @ \text{SiO}_2$ NPs immobilized by streptavidin (SA) for nucleic acid analysis has also been reported.

2. Materials and Methods

2.1 Materials

Analytical-grade chemicals were utilized throughout. Deionized (DI), double-distilled, and deoxygenated water was employed for the studies.

2.2 Methods

2.2.1 Preparation of Fe_3O_4 NPs

A solvothermal technique was used to synthesize Fe_3O_4 NPs. 40 mL of EG was used to dissolve 1.35 g of $\text{FeCl}_3 \cdot 6\text{H}_2\text{O}$. The addition of NaAc (1.8 g) and PEG 6000 (1.0 g) was done, and the mixture was vigorously stirred for 30 minutes. In our work, several concentrations of $\text{FeCl}_3 \cdot 6\text{H}_2\text{O}$, NaAc, and PEG

6000 were utilized. The blended solution's pH was changed from 5.4 to 10. The suspension were then enclosed in a stainless steel autoclave with Teflon lining and kept at 473 K for 8 hours before being cooled to room temperature. Under the influence of a magnetic field, the black precipitate was extracted from the reaction medium and washed twice with ethanol and three times with DI water. Fe₃O₄ NPs were finally re-dispersed in DI water. Using a transmission electronic microscope (TEM) (JEM2200CX, JEOL Ltd., Tokyo, Japan) operated at 200 kV, the size and shape of the materials was evaluated. Using a vibration sample magnetometer, magnetization measurements of Fe₃O₄ NPs were carried out at room temperature (VSM).

2.2.2 Synthesis of Fe₃O₄@SiO₂ nanoparticles

The produced Fe₃O₄ NPs were coated with SiO₂ shells by a slightly modified Stöber technique. In a typical procedure, 150 mL of a 75% ethanol/water solution containing 0.25 g of the previously generated Fe₃O₄ NPs were mixed gently for 3 hours at room temperature before adding 2.5 mL of tetraethoxysilane (TEOS) and 3 mL of ammonia. Under the influence of a magnetic field, the precipitate was removed from the reaction media and rinsed twice with ethanol and three times with DI water. In order to produce Fe₃O₄@SiO₂ NPs, the black powders were dried at 333 K for 6 hours. TEM was used to characterize the shape of Fe₃O₄@SiO₂ NPs as previously mentioned.

2.2.3 Preparation of SA-Modified Fe₃O₄@SiO₂ NPs

Similar to how it was previously reported, we synthesized SA-modified Fe₃O₄@SiO₂ NPs. Amino groups were initially added to Fe₃O₄@SiO₂ NPs using 3-aminopropyl triethoxysilane (APTS) and then aldehyde groups were added by a Schiff reaction involving the amino and aldehyde groups. After employing a magnetic wash in phosphate buffer (PB, 0.1 M, pH 7.0) to remove the excess glutaraldehyde from the NPs, the aldehyde-modified NPs were incubated with SA for an overnight duration. The ratio of NPs to SA was tuned. The amount of SA in the supernatant was measured using an ultraviolet spectrophotometer (Agilent 8453, Agilent Technologies, Inc., Santa Clara, CA, USA). The wavelength that was employed for detection was 595 nm. The amount of SA immobilized on those particles may then be calculated by subtracting the amount of SA present in Fe₃O₄@SiO₂ NPs. The SA-modified Fe₃O₄@SiO₂ NPs were washed and then re-dissolved in PB at a concentration of 4 mg/mL.

2.2.4 Capture of Biotin-Labeled Nucleic Acid on SA-Fe₃O₄@SiO₂ NPs

The nucleic acid sequence labeled with biotin at 5'-end and Cy3 fluorochrome at 3'-end was immobilized onto SA-Fe₃O₄@SiO₂ NPs through biotin-SA reaction. The oligonucleotide (5'-biotinTGAAGGAGAAGGTGTCTGCGGGA-Cy3-3') of methylene-tetra-hydrofolate reeducates (MTHFR) were used for measuring the amount of target nucleic acid fragment captured on SA-Fe₃O₄@SiO₂ NPs [35].

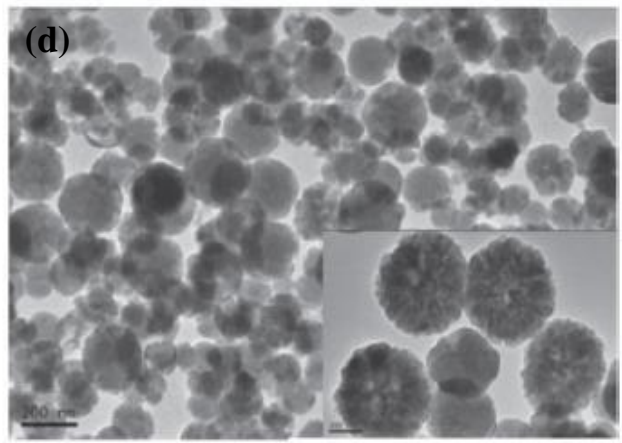
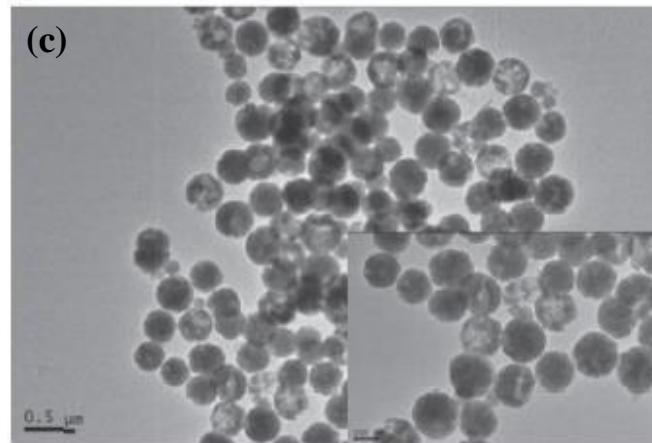
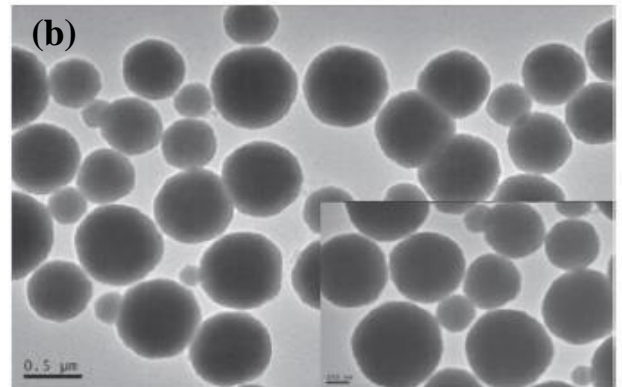
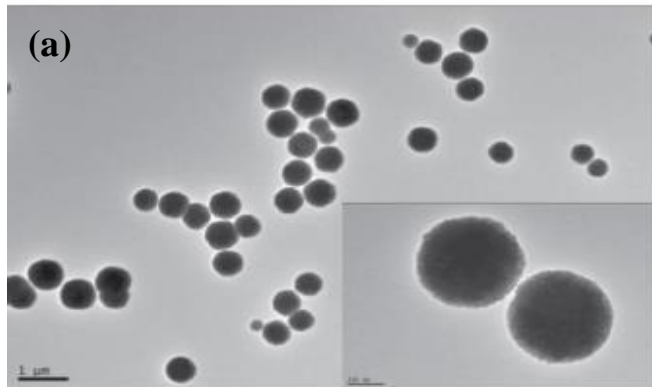
The NPs solution was gradually supplemented with desired nucleic acid concentrations throughout the ideal period of time at room temperature. Using a microarray scanner (GenePix 4100A, Molecular Devices, Inc.) at wavelengths of 635 nm for excitation and 675 nm for emission, the complexes of labeled nucleic acid fragment and NPs were separated magnetically, and the amount of target nucleic acid fragment that was not captured onto NPs was estimated in the supernatant.

By subtracting the quantity of non-caught target nucleic acid fragment from the total amount of inserted target nucleic acid fragment, the amount of target nucleic acid fragment captured on SA-Fe₃O₄@SiO₂ NPs could then be determined.

3 Results and Discussion

3.1 Diameter and Magnetic Properties of Fe₃O₄ and Fe₃O₄@SiO₂ NPs

Fe₃O₄ NPs of varied diameters tuned by Fe³⁺ concentration have been successfully synthesized, as reported by Cheng and colleagues. It follows naturally and logically that growing Fe³⁺ concentration led to an increase in NP diameter. TEM images of Fe₃O₄ magnetic NPs are shown in Fig. 1(a) Magnetic NPs created in a pH 5.4 environment, (b) Magnetic NPs created in a pH 5.5 environment, (c) Magnetic NPs created in a pH 5.6 environment, (d) Magnetic NPs created in a pH 5.7 environment, (e) Magnetic NPs created in a pH 5.8 environment, (f) Magnetic NPs created in a pH 5.9 environment, (g) Magnetic NPs created in a pH 6.0 environment, (h) Concentration of magnetic NPs produced under pH 10.0 conditions. Fe₃O₄ NPs were successfully synthesized by combining 1.35 g FeCl₃.6H₂O, 1.8 g NaAc, and 1.0 g PEG 6000 in 40 mL EG, then incubating the mixture at 473 K for 8 hours, as shown in Fig. 1. Except for the dosage of Fe³⁺, the dosages of NaAc and PEG 6000, temperature, and duration had no effect on the diameter of NPs. Our findings agreed with those of the study Cheng and colleagues presented. However, NPs' diameter was changed substantially by changing pH value of the starting combination (Table 1).



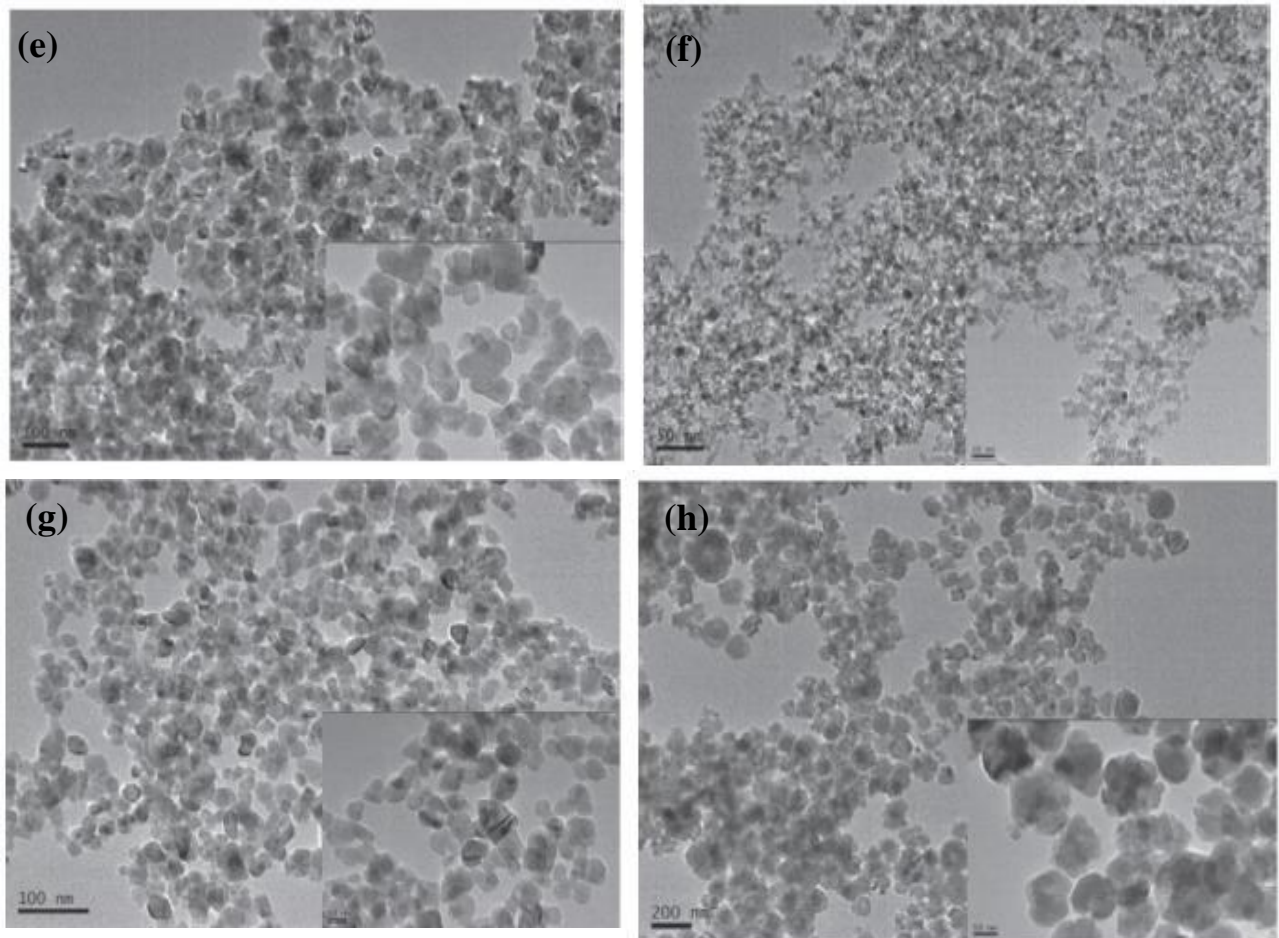


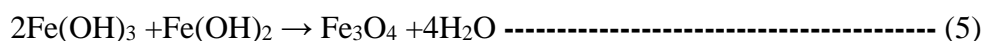
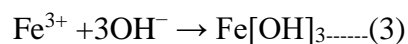
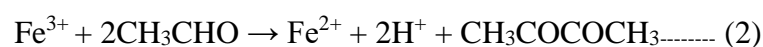
Fig. 1 TEM micrographs of Fe₃O₄ magnetic NPs (a), Magnetic NPs synthesized under pH 5.4 condition (b), Magnetic NPs synthesized under pH 5.5 condition (c), Magnetic NPs synthesized under pH 5.6 condition (d), Magnetic NPs synthesized under pH 5.7 condition (e) Magnetic NPs synthesized under pH 5.8 condition (f) Magnetic NPs synthesized under pH 5.9 condition, (g) Magnetic NPs synthesized under of pH 6.0 condition, (h) Magnetic NPs synthesized under pH 10.0 condition

Table I - Average diameter of Fe₃O₄ magnetic nanoparticles under different pH values

Name of the Figures	pH	Average diameter of NPs (nm)
Fig. 1(a)	5.4	642.29
Fig. 1(a)	5.5	450.75
Fig. 1(c)	5.6	338.88
Fig. 1(d)	5.7	133.23
Fig. 1(e)	5.8	85.79
Fig. 1(f)	5.9	24.92
Fig. 1(g)	6.0	21.78
Fig. 1(h)	10.0	10.28

The entire reaction took place inside of a holder, making it unable to adjust the solution's pH in real time. Therefore, the original reaction solution was the sole place where the pH value could be altered. The pH of the initial mixture, which was 5.4 without sodium hydroxide (NaOH), produced NPs with a diameter of around 600 nm [Fig. 1(a)]. With the addition of NaOH, the pH value rose from 5.4 to 5.8, which caused the diameters of the NPs to be tuned from 600 nm to 100 nm. The average NP diameter rapidly shrank to 20 nm when the pH level hit 6.0. As the pH level rose to 10.0, the average NP diameter shrank. Thus, it was proposed that the pH range of 5.4 to 6.0 has a significant impact on the diameter of the NPs'.

Solvothermal procedures have a milder redox reaction than co-precipitation techniques, which leads to good crystallization of the end products [36-37]. The hypothesized synthesis process in the current study system is explained as follows: Stage 1 involved the hydrolysis of EG and H₂O to yield acetaldehyde and hydroxyl and stage 2 involved the partial reduction of Fe(III) to Fe(II). Thus, by a redox reaction between Fe(III) and Fe(II) (stages [(3)–(5)], Fe₃O₄ NPs were created. Without additional hydroxyl, the process was relatively mild and the rate of nucleation was relatively moderate, which aided in the formation of NPs with good crystallization and a bigger diameter. In contrast, when additional hydroxyl was added, the rate of nucleation was sped up and the production of NPs with stable crystallization was simple and quick, leading to the production of NPs with reduced diameter. Therefore, a significant regulating factor of reaction rate that influenced the size and crystallization of artificial Fe₃O₄ NPs was solution pH.



The magnetic properties of the NPs in the various sizes listed in Table I, were also investigated using VSM. The saturation magnetization of NPs ranges from 31 to 85 emu/g. These results suggest that these NPs are ideal for usage as biological transporters and can be easily separated after a biological interaction. NPs with a diameter of 600 nm that were created at pH 5.4 without NaOH had a saturation magnetization of 51 emu/g. The maximum saturation magnetization 85 emu/g, was identified in NPs with a diameter of

around 300 nm, synthesized at pH 5.6. A minimal saturation magnetization of 31 emu/g was achieved by creating NPs with a diameter less than 10 nm at pH 10.0 conditions. For comparison with Figs. 1(a), 1(c), and 1(h), Fig. 2 shows the magnetic hysteresis loops of the initial, maximum, and minimum saturation magnetizations of Fe_3O_4 NPs (h). However, there was no discernible relationship between the magnetic properties and NPs sizes. According to published research, NPs' magnetic properties are mostly determined by their average grain size rather than their spherical diameter [6].

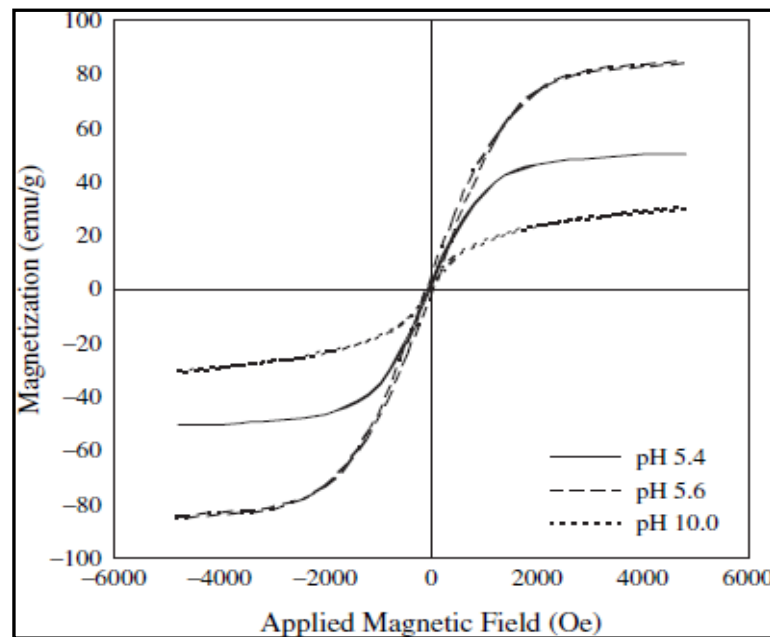


Fig. 2 Magnetic hysteresis loops of the magnetic NPs synthesized under pH 5.4, pH 5.6 and pH 10.0 conditions

3.2 Calculation of the Amount of Streptavidin Immobilized Onto SA- Fe_3O_4 @ SiO_2 NPs

The Fe_3O_4 NPs synthesized without additional NaOH were chosen to be used in the subsequent tests. A typical TEM picture of Fe_3O_4 NPs with a smooth silica layer is shown in Fig. 3(a). It is evident that the grey area is a SiO_2 shell and the dark dots are Fe_3O_4 NPs. Around the surface of each Fe_3O_4 NP, the light silica was uniformly deposited. The silica shell is around 100 nm thick, and the thickness might be adjusted by TEOS dosage according to the demands. Recently, Fe_3O_4 @ SiO_2 NPs with core-shell structures and excellent dispersibility have shown great interest to research for their unique physical and chemical properties and their many potential applications [38, 39]. Fe_3O_4 @ SiO_2 NPs can be conveniently

immobilized by SA. In our present study, we employed ultraviolet spectrophotometer to calculate the amount of SA bound to $\text{Fe}_3\text{O}_4@\text{SiO}_2$ NPs by covalent reaction. The capacity of SA on $\text{Fe}_3\text{O}_4@\text{SiO}_2$ NPs was investigated by mixing 300 g and gradient dosage of SA with mildly stirring for 30 min.

As shown in Fig. 3(b), the amount of SA immobilized on $\text{Fe}_3\text{O}_4@\text{SiO}_2$ NPs increased with the increase in SA dosage until it was saturated when more than 9 g SA was introduced for covalent interaction. The maximal amount of SA immobilized onto the $\text{Fe}_3\text{O}_4@\text{SiO}_2$ NPs was 29.3 g/mg. Therefore, the ratio used in the following experiment was determined as 30 g/mg (SA/ $\text{Fe}_3\text{O}_4@\text{SiO}_2$ NPs), the optimal ratio by TEOS dosage according to the demands. Recently, $\text{Fe}_3\text{O}_4@\text{SiO}_2$ NPs with core-shell structures and excellent dispersibility have shown great interest to research for their unique physical and chemical properties and their many potential applications [38, 39].

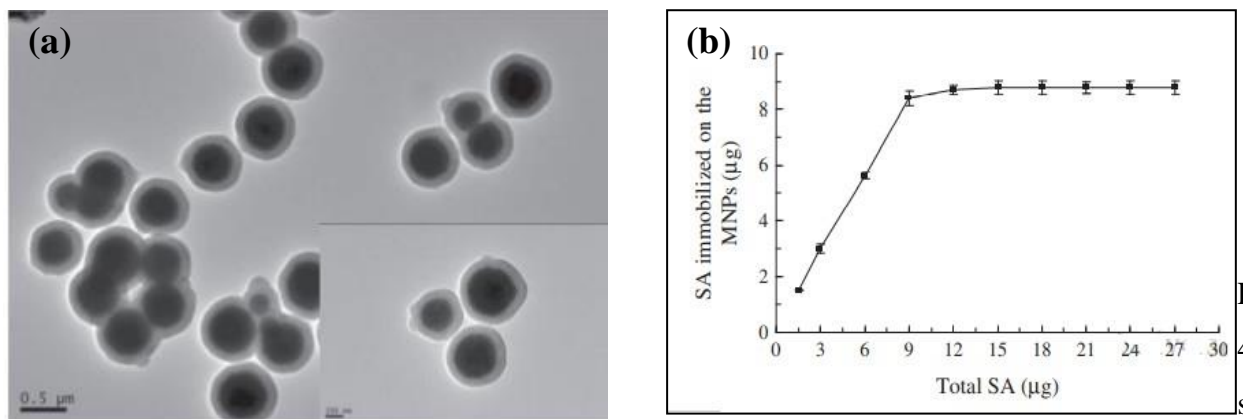


Fig. 3
4
sho

As shown in Fig. 3(b), the amount of SA immobilized on $\text{Fe}_3\text{O}_4@\text{SiO}_2$ NPs increased with the increase in SA dosage until it was saturated when more than 9 g SA was introduced for covalent interaction. The maximal amount of SA immobilized onto the $\text{Fe}_3\text{O}_4@\text{SiO}_2$ NPs was 29.3 g/mg. Therefore, the ratio used in the following experiment was determined as 30 g/mg (SA/ $\text{Fe}_3\text{O}_4@\text{SiO}_2$ NPs) as the optimal ratio.

As shown in Fig. 3(b), the amount of SA immobilized on $\text{Fe}_3\text{O}_4@\text{SiO}_2$ NPs increased with the increase in SA dosage until it was saturated when more than 9 g SA was introduced for covalent interaction. The maximal amount of SA immobilized onto the $\text{Fe}_3\text{O}_4@\text{SiO}_2$ NPs was 29.3 g/mg. Therefore, the ratio used in the following experiment was determined as 30 g/mg (SA/ $\text{Fe}_3\text{O}_4@\text{SiO}_2$ NPs) as the optimal ratio.

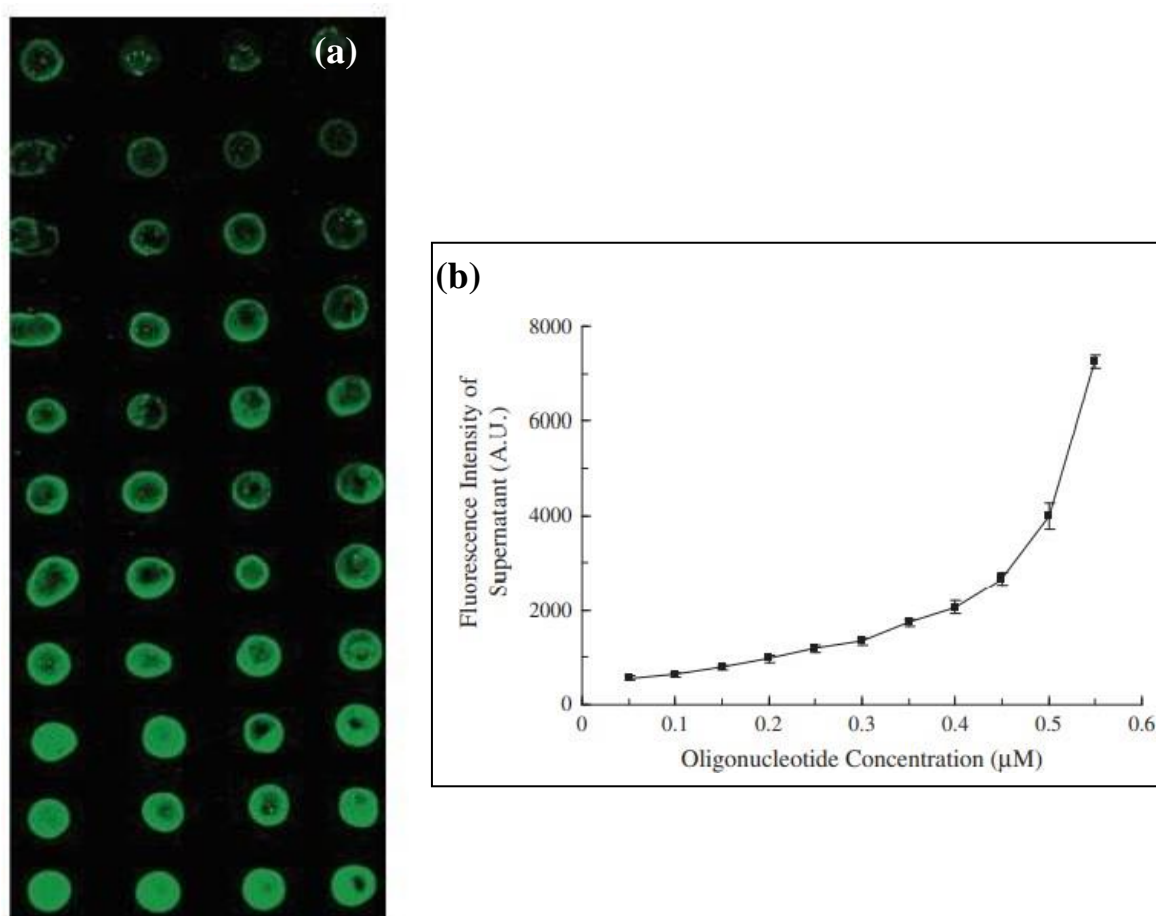


Fig. 4 Capture of target oligonucleotides on streptavidin modified $\text{Fe}_3\text{O}_4@\text{SiO}_2$ by covalent reaction, (a) Fluorescence intensities in the supernatant with addition of different concentrations of 5-biotin/3-Cy3-labeled oligonucleotides, (b) Fluorescence intensity values in the supernatant with addition of different concentrations of 5-biotin/3-Cy3-labeled oligonucleotides

3.3 Capture of Oligonucleotide on SA- $\text{Fe}_3\text{O}_4@\text{SiO}_2$ NPs

The amount of target DNA captured on SA- $\text{Fe}_3\text{O}_4@\text{SiO}_2$ NPs was assessed using 5-biotin/3 - Cy3-labeled oligonucleotides since the amount of biotin labeled target DNA collected on SA- $\text{Fe}_3\text{O}_4@\text{SiO}_2$ NPs greatly affected the sensitivity for DNA analysis. 40 Gradient concentrations of biotin-labeled targets were added to a solution containing 100 g of SA- $\text{Fe}_3\text{O}_4@\text{SiO}_2$ NPs in order to maximize the binding efficiency of nucleic acid fragments. The saturated amount of the biotin-labeled oligonucleotides was calculated by measuring the fluorescence intensity in the supernatant. Fig. 5 shows the Time vs Fluorescence Intensities plots of SA immobilized onto modified $\text{Fe}_3\text{O}_4@\text{SiO}_2$.

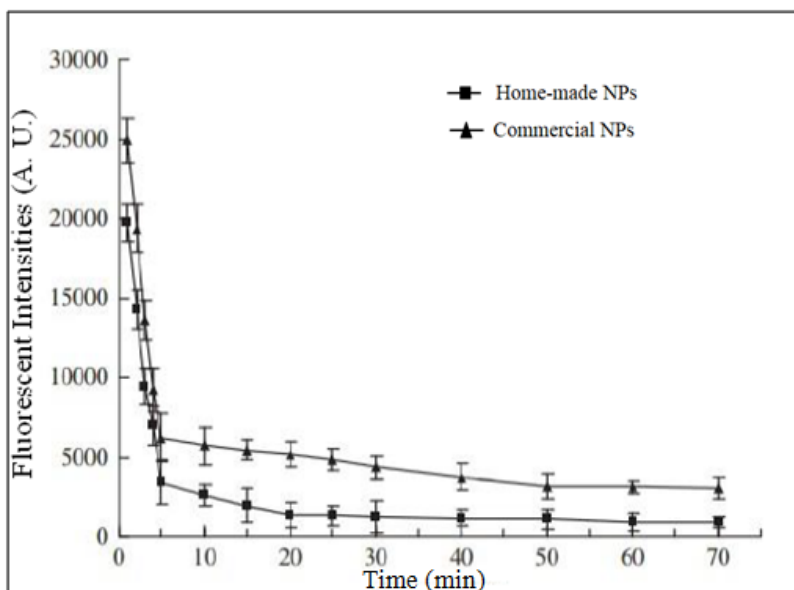


Fig. 5 Reaction time optimization of streptavidin immobilized onto modified $\text{Fe}_3\text{O}_4@\text{SiO}_2$

4 Conclusion

Fe_3O_4 and $\text{Fe}_3\text{O}_4@\text{SiO}_2$ NPs have various particular characteristics, for example, a steady center shell structure, a high unambiguous surface region, and a surface that is effectively modifiable. In this paper, it has been reported that solvothermal-assisted Fe_3O_4 NPs with customizable pH were successfully produced with a controllable measurement. The consideration of antacid is remembered to have sped up and made the redox response among Fe(II) and Fe(III) in the framework more serious. The scope of 31-85 emu/g was the great soaked polarization of all Fe_3O_4 NPs that were promptly accessible. $\text{Fe}_3\text{O}_4@\text{SiO}_2$ NPs were successfully synthesized utilizing the customary modified Stöber process, and in light of their high SA immobilization, they made great attractive transporters for nucleic corrosive discovery.

5. References

1. H. Chen, C. Deng, and X. Zhang, *Angew. Chem. Int. Ed. Engl.* 49, 607 (2010).
2. E. G. Xiong and S. L. Wang, *Int. J. Appl. Electromagn. Mech.* 13, 445 (2009).
3. A. Arkhis, A. Elaissari, T. Delair, B. Verrier, and B. Mandrand, *J. Biomed. Nanotechnol.* 6, 28 (2010).

4. M. Naresh, M. Sharma, and A. Mittal, *J. Biomed. Nanotechnol.* 7, 572 (2011).
5. D. Šponarová, D. Horák, M. Trchová, P. Jendelová, V. Herynek, N. Mitina, A. Zaichenko, R. Stoika, P. Lesný, and E. Syková, *J. Biomed. Nanotechnol.* 7, 384 (2011).
6. X. Gao, B. Kan, M. Gou, J. Zhang, G. Guo, N. Huang, X. Zhao, and Z. Qian, *J. Biomed. Nanotechnol.* 7, 285 (2011).
7. S. R. Dave and X. Gao, *Rev. Nanomed. Nanobiotechnol.* 1, 583 (2009).
8. A. Elias and A. Tsourkas, *Hematology* 1, 720 (2009).
9. C. Xu and S. Sun, *Dalton. Trans.* 7, 5583 (2009).
10. X. Peng, L. Manna, W. Yang, J. Wickham, E. Scher, A. Kadavanich, and A. P. Alivisatos, *Nature* 404, 59 (2000).
11. V. F. Puentes, K. M. Krishnan, and A. P. Alivisatos, *Science* 291, 2115 (2001).
12. S. P. Singh, *J. Biomed. Nanotechnol.* 7, 95 (2011).
13. K. W. Huang, S. Y. Yang, C. Y. Yu, J. J. Chieh, C.-C. Yang, H.-E. Horng, and C.-Y. Hong, *J. Biomed. Nanotechnol.* 7, 535 (2011).
14. S. Sun, H. Zeng, D. B. Robinson, S. Raoux, P. M. Rice, S. X. Wang, and G. Li, *J. Am. Chem. Soc.* 126, 273 (2004).
15. L. He, Z. Li, J. Fu, Y. Deng, N. He, Z. Wang, H. Wang, and Z. Shi, *J. Biomed. Nanotechnol.* 5, 596 (2009).
16. K. Men, S. Zeng, M. L. Gou, G. Guo, Y. C. Gu, F. Luo, X. Zhao, Y. Q. Wei, and Z. Y. Qian, *J. Biomed. Nanotechnol.* 6, 287 (2010).
17. D. Kim, N. Lee, M. Park, B. H. Kim, K. An, and T. Hyeon, *J. Am. Chem. Soc.* 131, 454 (2009).
18. D. Srikala, V. N. Singh, A. Banerjee, and B. R. Mehta, *J. Nanosci. Nanotechnol.* 10, 8088 (2010).
19. L. Suber, P. Imperatori, G. Ausanio, F. Fabbri, and H. Hofmeister, *J. Phys. Chem. B.* 109, 7103

(2005).

20. K. K. Ostrikov, I. Levchenko, U. Cvelbar, M. Sunkara, and M. Mozetic, *Nanoscale* 2, 2012 (2010).
21. F. L. Yuan, X. Wang, P. Hu, L. J. Yu, and L. Y. Bai, *J. Phys. Chem. C* 112, 8773 (2008).
22. Z. Y. Huang, Y. F. Li, Y. Mi, and J. Y. Jiang, *Chem. Lett.* 39, 760 (2010).
23. B. Geng, F. Zhan, H. Jiang, Y. Guo, and Z. Xing, *Chem. Commun.* 30, 5773 (2008).
24. S. Ilbasemis-Tamer, S. Yilmaz, E. Banoglu, and I. T. Degim, *J. Biomed. Nanotechnol.* 6, 20 (2010).
25. M. J. Hu, Y. Lu, S. Zhang, S. R. Guo, B. Lin, M. Zhang, and S. H. Yu, *J. Am. Chem. Soc.* 130, 11606 (2008).
26. B. Lv, Y. Xu, Q. Gao, D. Wu, and Y. Sun, *J. Nanosci. Nanotechnol.* 10, 2348 (2010).
27. D. R. Chen, J. Lu, X. L. Jiao, and W. Li, *J. Phys. Chem. C* 113, 4012 (2009).
28. H. T. Kim, Q. Lu, K. J. Lee, S. J. Hong, N. V. Myung, and Y. H. Choa, *J. Nanosci. Nanotechnol.* 10, 3393 (2010).
29. Y. Zeng, R. Hao, B. Xing, Y. Hou, and Z. Xu, *Chem. Commun.* 46, 3920 (2010).
30. S. Kundu and H. Liang, *J. Nanosci. Nanotechnol.* 10, 746 (2010).
31. Y. Cheng, R. Q. Tan, W. Y. Wang, Y. Q. Guo, P. Cui, and W. J. Song, *J. Mater. Sci.* 45, 5347 (2010).
32. K. G. Sung, S.-B. Choi, and M. K. Park, *Adv. Sci. Lett.* 4, 805 (2011).
33. Z. Wang, Y. Guo, S. Li, Y. Sun, and N. He, *J. Nanosci. Nanotechnol.* 8, 1797 (2008).
34. Z. Y. Li, L. He, N. Y. He, Y. Deng, Z. Y. Shi, H. Wang, S. Li, H. N. Liu, Z. F. Wang, and D. X. Wang, *J. Nanosci. Nanotechnol.* 11, 1074 (2011).
35. S. Li, H. Liu, and N. He, *J. Nanosci. Nanotechnol.* 10, 4875 (2010).
36. A. Shukla, M. K. Patra, M. Mathew, S. Songara, V. K. Singh, G. S. Gowd, S. R. Vadera, and

N. Kumar, Adv. Sci. Lett. 3, 161 (2010).

37. R. Liu and L. Wang, Adv. Sci. Lett. 4, 814 (2011).

38. Z. Y. Li, L. He, N. Y. He, Z. Y. Shi, H. Wang, S. Li, H. N. Liu, X. L. Li, Y. B. Dai, and Z. F. Wang, J. Nanosci. Nanotechnol. 10, 696 (2010).

39. H. Y. Lin, W. Y. Chen, and Y. C. Chen, J. Biomed. Nanotechnol. 5, 215 (2009).

40. L. Mair, K. Ford, M. R. Alam, R. Kole, M. Fisher, and R. Superfine, J. Biomed. Nanotechnol. 5, 182 (2009).

41. Y. Deng, D. Qi, C. Deng, X. Zhang, and D. Zhao, J. Am. Chem. Soc. 130, 28 (2008).

42. H. N. Liu, S. Li, L. Tian, L. S. Liu, and N. Y. He, J. Nanosci. Nanotechnol. 10, 5311 (2010).

43. M. Chanana, Z. W. Mao, and D. Y. Wang, J. Biomed. Nanotechnol. 5, 652 (2009).